Neuron, Vol. 15, 1065–1076, November, 1995, Copyright © 1995 by Cell Press

# Amplification of EPSPs by Axosomatic Sodium Channels in Neocortical Pyramidal Neurons

**Greg Stuart and Bert Sakmann**
Abteilung Zellphysiologie
Max-Planck-Institut für medizinische Forschung
Jahnstrasse 29
69120 Heidelberg
Federal Republic of Germany

## Summary

**Simultaneous somatic and dendritic recordings were made from the same neocortical layer V pyramidal neuron, and current injection via the dendritic recording pipette was used to simulate the voltage change that occurs during an EPSP. At the soma, these simulated EPSPs increased nonlinearly with the amplitude of the dendritic current injection and with depolarization of the membrane potential. Bath application of the sodium channel blocker TTX decreased large (>5 mV) EPSPs and also blocked amplification of EPSPs at depolarized membrane potentials, whereas calcium channel blockers had little effect. Local application of TTX to the soma and axon blocked EPSP amplification, whereas dendritic application had little effect. Simultaneous somatic and axonal recordings demonstrated that EPSP amplification was largest in the axon. These results show that EPSPs are amplified by voltage-activated sodium channels located close to the soma and in the axon.**

## Introduction

Excitatory postsynaptic potentials (EPSPs) in neocortical pyramidal neurons must spread to the site of action potential generation, in the axon (Stuart and Sakmann, 1994), before their summation can lead to action potential initiation. In a passive dendritic tree, these EPSPs will be attenuated in amplitude and slowed in time course as they spread to the soma (Rall, 1977), suggesting that excitatory synapses located on distal dendrites will be less effective in depolarizing the neuron to action potential threshold than those located more proximally. Dendrites of neocortical pyramidal neurons, however, contain voltage-activated sodium and calcium channels (Huguenard et al., 1989; Amitai et al., 1993; Kim and Connors, 1993; Regehr et al., 1993; Markram and Sakmann, 1994; Stuart and Sakmann, 1994; Yuste et al., 1994; Markram et al., 1995; Schiller et al., 1995), which could increase the amplitude of EPSPs (see Jack et al., 1983; Miller et al., 1985; Perkel and Perkel, 1985; Cauller and Connors, 1992; De Schutter and Bower, 1994; Bernander et al., 1994). For this to occur, an EPSP must be of sufficient amplitude to activate (or deactivate) voltage-dependent channels operating at membrane potentials below action potential threshold. EPSP amplification could occur at the resting membrane potential (RMP) or may require prior de- or hyperpolarization and could occur near the site of EPSP generation (i.e., in the dendritic spine or the adjacent dendrite) or during spread of the EPSP to the site of action potential initiation.

An increase in amplitude and duration of EPSPs in neocortical pyramidal neurons has previously been observed during depolarization of the membrane potential (Stafstrom et al., 1985; Thomson et al., 1988; Sutor and Hablitz, 1989a, 1989b; Deisz et al., 1991; Hirsch and Gilbert, 1991). One possible explanation for this effect is that at depolarized membrane potentials these EPSPs activate voltage-dependent sodium or calcium channels (Stafstrom et al., 1985; Sutor and Hablitz, 1989b; Deisz et al., 1991; Hirsch and Gilbert, 1991). Another possibility is that postsynaptic depolarization leads to recruitment of synaptic N-methyl-D-aspartate (NMDA) receptor channels blocked at more hyperpolarized potentials by extracellular magnesium (Jones and Baughman, 1988; Thomson et al., 1988; Artola and Singer, 1990; but see Deisz et al., 1991; Hirsch and Gilbert, 1991). One of the difficulties in distinguishing between these possibilities, and in general in determining whether voltage-dependent channels are activated (or deactivated) by subthreshold EPSPs, is that the application of blockers of postsynaptic voltage-activated channels will in most cases modify or block synaptic transmission.

The aim of the experiments described in this paper was to determine whether subthreshold EPSPs in neocortical layer V pyramidal neurons can be amplified by voltage-activated channels. This was investigated through the use of a novel technique: simultaneous somatic and dendritic current-clamp recordings were made from the same neocortical pyramidal neuron, and the voltage change during an EPSP was simulated by dendritic current injection with a time course similar to that of an excitatory postsynaptic current (EPSC). These "simulated EPSPs" were then recorded both at their site of generation in the dendrites and at the soma, and the effect of application of blockers of voltage-activated channels was determined. Using this approach, it was possible to examine both the conditions and the mechanisms by which subthreshold EPSPs in neocortical pyramidal neurons can be amplified by voltage-activated channels.

## Results

Experiments were performed on visually identified, large layer V pyramidal neurons in brain slices from somatosensory cortex of 14- to 28-day-old rats. In 28-day-old rats, the average somatic action potential amplitude (measured from threshold) was 95.2 ± 2.0 mV, action potential half width and maximum rate of rise were 0.57 ± 0.02 ms and 512 ± 41 V/s, respectively, and action potential threshold was on average 13.6 ± 0.6 mV depolarized from the somatic RMP (−64.1 ± 0.8 mV; n = 13). Note that membrane potential measurements were not corrected for the junction potential between the bath and pipette solutions.

These basic electrophysiological properties are very

similar to those previously reported for adult large layer V pyramidal neurons (see Stafstrom et al., 1984; Mason and Larkman, 1990). In addition, action potential burst firing, typical of that seen in large layer V pyramidal neurons (see Mason and Larkman, 1990; Chagnac-Amitai et al., 1990), was observed in 69% of cells in 28-day-old rats. No bursting was observed in 14-day-old animals, consistent with the findings of Kasper et al. (1994), who, using an external potassium concentration similar to that used in our experiments, noted that action potential burst firing in rat layer V pyramidal neurons is not fully developed until 3–4 weeks of age.

### Generation of Simulated EPSPs

Simulated EPSPs were generated by dendritic current injection into the apical dendrite of layer V pyramidal neurons during simultaneous somatic and dendritic recording. The time course of this current injection was based on the kinetics of spontaneous EPSCs, which were selected for their fast rise times (<0.5 ms) during low access resistance somatic whole-cell recordings (Figure 1A; see Experimental Procedures). These spontaneous EPSCs had an average amplitude of 15.5 ± 1.7 pA and a rise time (20%–80%) of 0.32 ± 0.02 ms, and their decay could be well fit by a single exponential with a time constant of 3.3 ± 0.3 ms (Figure 1A; average from 4 cells). Using these values, a waveform was constructed with a single exponential rise and decay, such that the 20%–80% rise time was 0.3 ms and the decay time constant was 3 ms. The voltage response at the soma or dendrite following dendritic current injection with this time course was used to simulate an EPSP.

A comparison of evoked and simulated EPSPs recorded in the same cell is shown in Figure 1B. In this example, the simulated EPSP was generated by dendritic current injection 420 μm from the soma, and the evoked EPSP was generated by extracellular stimulation close to the dendritic recording pipette (<50 μm). The time courses of the simulated and evoked EPSPs recorded at the same somatic and dendritic locations were similar. The average rise time and half width of small (<5 mV) evoked EPSPs at the soma were 2.3 ± 0.2 ms and 16.5 ± 0.7 ms, respectively (n = 6; 28-day-old rats). Simulated EPSPs of a similar amplitude at the soma of the same cells had average rise times and half widths of 2.7 ± 0.1 ms and 14.6 ± 0.4 ms, respectively (simulated EPSPs in these experiments were generated by dendritic current injections 390–580 μm from the soma). When evoked EPSPs were generated close to the dendritic recording pipette (as judged by their fast rise time), the time courses of evoked and simulated EPSPs at the dendritic recording site were also similar (Figure 1B). In these cases, evoked EPSPs recorded in the dendrites had an average rise time of 0.7 ± 0.12 ms and an average half width of 8.4 ± 0.8 ms (n = 4). Simulated EPSPs recorded at the same dendritic locations in the same cells had an average rise time of 0.6 ± 0.02 ms and and average half width of 6.6 ± 0.3 ms. Note that both evoked and simulated dendritic EPSPs decay faster than somatic EPSPs, and that the decay of both somatic and dendritic EPSPs undershoots a baseline set at the RMP (Figure 1B).

### Effects of EPSP Amplitude

An example of the effect of EPSP amplitude on the time course of evoked and simulated EPSPs recorded at the soma of the same cell is shown in Figure 2A. The amplitude of EPSPs was changed by altering the stimulus strength for evoked EPSPs or the size of the dendritic current injection for simulated EPSPs. As evoked and simulated EPSP amplitude increased, the EPSP time to peak and duration became longer. This effect can be seen more clearly when small (<5 mV) and large (>10 mV) EPSPs at the soma were averaged and normalized to the same amplitude (Figure 2B). For evoked EPSPs, this was not due to the recruit-

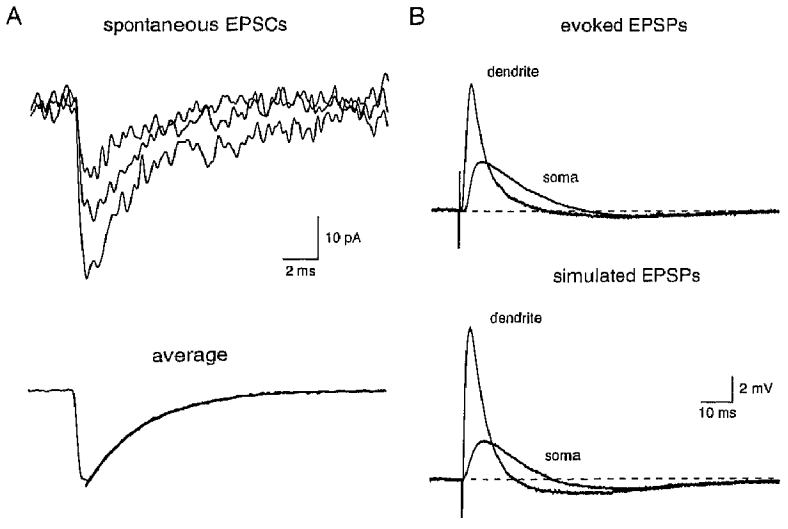


Figure 1. Generation of Simulated EPSPs

(A) Top: EPSCs recorded from the soma at the resting membrane potential (RMP; −62 mV) in the presence of bicuculline to block $GABA_A$ receptor-mediated events. Bottom: Average of 200 of these spontaneous EPSCs selected for their fast rise times (20%–80% rise times < 0.5 ms) and uniform decays. The 20%–80% rise time of this average EPSC was 0.3 ms, and its decay was fitted with a single exponential with a time constant of 3.2 ms (thick line).

(B) Comparison of evoked (top) and simulated (bottom) EPSPs recorded simultaneously at the soma and the site of EPSP generation in the dendrites (420 μm from the soma). Synaptically evoked EPSPs were generated by extracellular stimulation close to the dendritic recording pipette (<50 μm), and simulated EPSPs were evoked by injection of a 1 nA exponentially rising and decaying waveform ($\tau_{on}$ = 0.3 ms; $\tau_{off}$ = 3 ms) via the dendritic recording pipette. Recordings were made at the somatic and dendritic RMP (both −65 mV). The transient before the evoked EPSPs is the stimulus artifact, and the downward transient before the simulated dendritic EPSP is the capacitive transient associated with the dendritic current injection used to generate this EPSP. Note that this capacitive transient distorts the initial rising phase of the measured voltage change during the dendritic simulated EPSP.

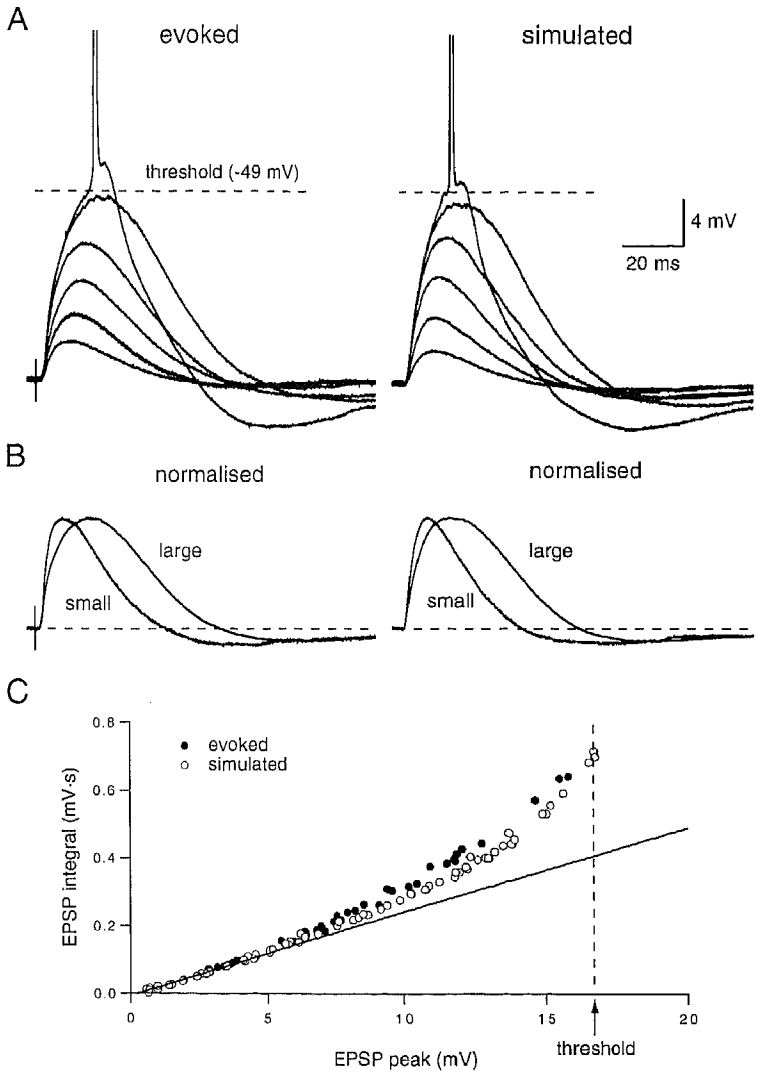


Figure 2. Effects of a Change in EPSP Amplitude on Evoked and Simulated EPSPs

(A) Comparison of evoked (left) and simulated (right) EPSPs recorded at the soma of the same cell at the RMP (−66 mV) during an increase in stimulus intensity for evoked EPSPs or in the size of the dendritic current injection for simulated EPSPs. Simulated EPSPs were generated by dendritic current injections of different amplitudes 365 μm from the soma. The action potential threshold is indicated by the dotted line (−49 mV).

(B) Small (<5 mV) and large (>10 mV) evoked (left) and simulated (right) EPSPs were averaged and normalized to the same amplitude (same cell as in [A]).

(C) The peak amplitudes of evoked (closed circles) and simulated (open circles) EPSPs at the soma were plotted against their integrals during a change in EPSP amplitude. The solid line is the linear regression fit to the data for EPSPs with amplitudes of <5 mV (data from same cell as in [A]). The action potential threshold is indicated by the dotted line.

ment of NMDA receptors by the largest EPSPs or to a change in the amount of inhibition with stimulus strength, as it was observed both in the absence and presence of the NMDA and γ-aminobutyric acid type A ($GABA_A$) receptor blockers DL-2-amino-5-phosphonopentanoic acid (APV) and bicuculline (n = 6). The change in EPSP time course as the amplitude of EPSPs is increased can be seen graphically by plotting the EPSP peak amplitude against its integral (Figure 2C; EPSP integral was defined as the area under the EPSP above a baseline set at the RMP). In most cases this relationship deviated from linearity, with the EPSP integral increasing more than the EPSP peak for EPSPs at the soma with amplitudes greater than ~5 mV. The similarity in the changes in evoked and simulated EPSPs during an increase in EPSP amplitude suggests that postsynaptic voltage-activated channels are involved in shaping the time course of EPSPs with amplitudes greater than ~5 mV. In addition, this finding also shows that the simulated EPSPs adequately mimic the effects of a change in evoked EPSP amplitude.

**Effects of Membrane Potential**

The effects of changes in the membrane potential on both evoked and simulated EPSPs recorded from the soma of the same cell are shown in Figure 3A. As the membrane potential becomes more depolarized, the somatic amplitude, time to peak, and integral of small (<5 mV) evoked and simulated EPSPs increased. For evoked EPSPs this increase was not due to recruitment of NMDA receptors or to changes in inhibition, as in these experiments NMDA and $GABA_A$ receptors were blocked. When the effect of membrane potential depolarization on evoked EPSPs in the absence and presence of the NMDA receptor blocker APV was examined, it was found that the addition of APV had little if any effect on the increase in EPSP amplitude or integral observed at subthreshold depolarized membrane potentials (n = 3; see also Deisz et al., 1991; Hirsch and Gilbert, 1991). The largest increase in evoked and simulated EPSPs occurred at membrane potentials closest to the action potential threshold, with the timing of action potential initiation after the onset of both evoked and simu-

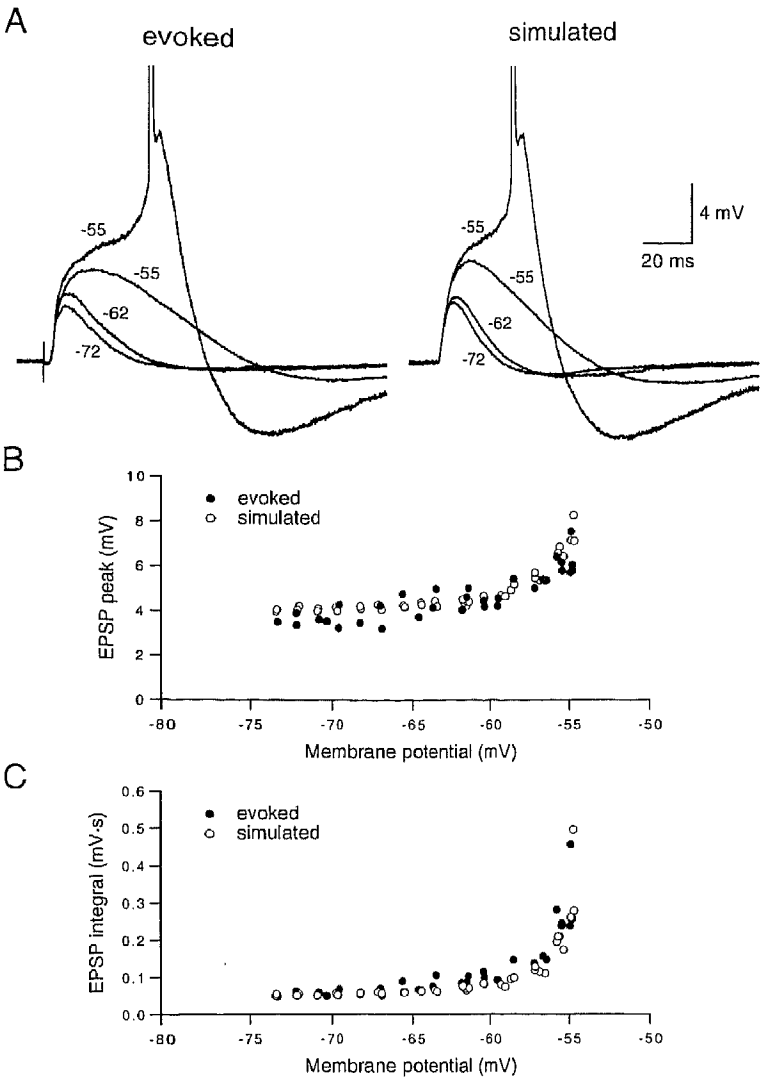


Figure 3. Effects of a Change in Membrane Potential on Evoked and Simulated EPSPs

(A) Comparison of evoked (left) and simulated (right) EPSPs recorded at the soma of the same cell at the indicated membrane potentials. Simulated EPSPs were generated by 1.5 nA dendritic current injections 380 μm from the soma. The somatic RMP was −64 mV, and action potentials were initiated by these EPSPs at somatic membrane potentials of −55 mV.

(B) The peak amplitudes of evoked (closed circles) and simulated (open circles) EPSPs at the soma are plotted against the membrane potentials at which the data were recorded (data from same cell as in [A]).

(C) The integrals of evoked (closed circles) and simulated (open circles) EPSPs at the soma are plotted against the membrane potentials at which the data were recorded (data from same cell as in [A]).

lated EPSPs being dependent on the time course of EPSP amplification (Figure 3A). In any one neuron, evoked and simulated EPSPs were amplified to similar extents by membrane depolarization, with a greater increase in EPSP integral than in EPSP peak (Figures 3B and 3C). On average, in comparison with EPSP amplitude and integral at the RMP, at the most depolarized subthreshold membrane potentials, EPSP peak amplitude increased ~2-fold, whereas EPSP integral increased 4- to 5-fold (n = 15). The similarity in the effect of membrane potential on evoked and simulated EPSPs suggests that activation of postsynaptic voltage-dependent channels mediates this form of EPSP amplification and also shows that the effect of a change in membrane potential on evoked EPSPs can be mimicked by the simulated EPSPs.

**Differential Effects on Somatic and Dendritic EPSPs**

An example of the effect of progressively increasing the size of the dendritic current injection on somatic and dendritic simulated EPSPs is shown in Figure 4A. The peak amplitude and integral of somatic EPSPs and the integral of dendritic EPSPs increased nonlinearly with the size of the dendritic current injection, whereas the amplitude of dendritic EPSPs increased linearly (Figures 4B and 4C). Similar observations were made in 10 other cells. Note that the nonlinear increase in somatic EPSP amplitude and somatic and dendritic EPSP integral occurred only for EPSPs with amplitudes greater than ~5 mV at the soma.

These results show that both the integral and peak of large (>5 mV) somatic simulated EPSPs are increased in a nonlinear manner as the size of the dendritic injected current is increased, suggesting that these EPSPs are amplified by voltage-activated channels. Conversely, the linear increase in the dendritic EPSP peak suggests that the amplification of somatic EPSPs is not associated with amplification of the dendritic EPSP peak. Note that, as the size of the dendritic current injection was increased, there was usually a larger nonlinear increase in the somatic EPSP integral than in the peak (compare Figures 4B and 4C). This differential increase in somatic EPSP peak amplitude and integral can account for the increased

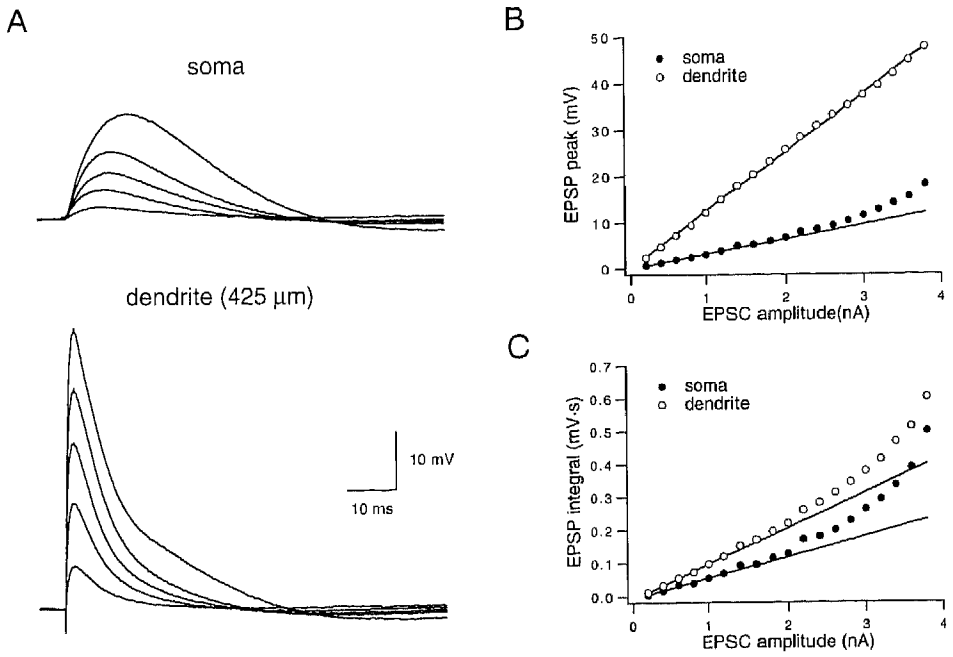


Figure 4. Effects of a Change in EPSP Amplitude on Somatic and Dendritic Simulated EPSPs

(A) Comparison of somatic (top) and dendritic (bottom) simulated EPSPs recorded simultaneously at the RMP (soma, −68 mV; dendrite, −67 mV) during an increase in the size of the dendritic current injection. Simulated EPSPs were generated by 0.6, 1.4, 2.2, 3.0, and 3.8 nA dendritic current injections 425 μm from the soma.

(B) The peak amplitudes of somatic (closed circles) and dendritic (open circles) simulated EPSPs are plotted against the size of the dendritic current injections (data are from same cell as in [A]). The lines are linear regression fits to the somatic and dendritic data for EPSPs of <5 mV in amplitude for the somatic data and for all EPSPs for the dendritic data.

(C) The integrals of somatic (closed circles) and dendritic (open circles) simulated EPSPs are plotted against the size of the dendritic current injections (data from same cell as in [A]). The lines are linear regression fits to the somatic and dendritic data for events where the EPSP at the soma was <5 mV in amplitude.

duration of large somatic EPSPs (see Figure 2B) and the nonlinear shape of somatic EPSP peak versus integral plots like those shown in Figure 2C.

The effect of a change in membrane potential on somatic and dendritic EPSPs is shown in Figure 5. As the somatic and dendritic membrane potentials were depolarized, both the amplitude and duration of small (<5 mV) somatic EPSPs increased. This effect, however, was not associated with an increase in the amplitude of the dendritic EPSP (Figure 5A). In addition, a noticeable hump developed during the decay of the dendritic EPSPs (Figure 5A, lower −55 mV trace). This hump was largest at the most depolarized membrane potentials, and when somatic and dendritic EPSPs were superimposed, it was clear that the amplitude of this hump was largest at the soma (n = 7; data not shown). A similar observation was made for evoked EPSPs (n = 5). Subtraction of somatic and dendritic EPSPs recorded at the RMP from those at the most depolarized subthreshold membrane potentials revealed that the conductance change underlying amplification of EPSPs had a slow time course and was largest at the soma (Figure 5B). The effects of a change in membrane potential on somatic and dendritic EPSP peak amplitude and integral are shown graphically in Figures 5C and 5D. While both the peak and integral of somatic EPSPs and the integral of dendritic EPSPs increased with depolarization of the membrane potential, the peak of dendritic EPSPs was unchanged (Figures 5C and 5D). Similar results were observed in 7 other cells.

In summary, these results suggest that the conductance change underlying the amplification of somatic EPSPs has a slow time course and is not associated with amplification of the peak of the dendritic EPSP. Furthermore, the site of EPSP amplification is likely to be close to the soma, where amplification is greatest.

### Effect of the Sodium Channel Blocker TTX on Simulated EPSPs

Bath application of tetrodotoxin (TTX; 0.5 or 1 μM) was used to determine whether voltage-activated sodium channels are involved in the amplification of simulated EPSPs. TTX caused a substantial reduction in the amplitude and integral of somatic EPSPs with amplitudes greater than ~5 mV (Figures 6A and 6B; n = 9). In addition, the application of TTX "linearized" the relationship between somatic EPSP amplitude and integral and the size of the current injection used to generate simulated EPSPs (Figure 6B). The effect of TTX was greater on EPSP integral than on EPSP peak amplitude, decreasing the peak amplitude of the largest subthreshold EPSPs by 29% ± 2% and their integral by 53% ± 5% (n = 9).

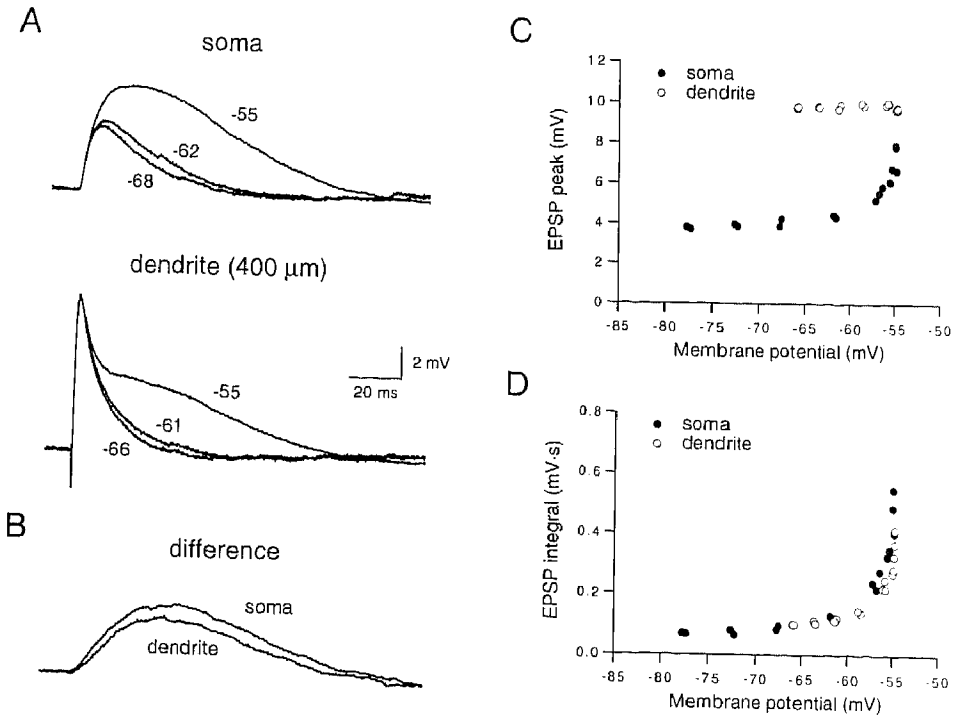


Figure 5. Effects of a Change in Membrane Potential on Somatic and Dendritic Simulated EPSPs

(A) Comparison of somatic (top) and dendritic (bottom) simulated EPSPs recorded at the indicated membrane potentials. Simulated EPSPs were generated by 1 nA dendritic current injections 400 μm from the soma, and the somatic and dendritic membrane potential was changed by somatic current injection. The somatic and dendritic RMPs were −63 mV and −60 mV, respectively.

(B) Somatic and dendritic simulated EPSPs at the RMP were subtracted from EPSPs recorded at the most depolarized subthreshold membrane potentials and overlaid (same cell as in [A]).

(C) The peak amplitudes of somatic (closed circles) and dendritic (open circles) simulated EPSPs are plotted against the membrane potentials at which the data were recorded (data from same cell as in [A]).

(D) The integrals of somatic (closed circles) and dendritic (open circles) simulated EPSPs are plotted against the membrane potentials at which the data were recorded (data from same cell as in [A]).

TTX also linearized somatic EPSP peak amplitude versus integral plots like those shown in Figure 2C (n = 9). In contrast to its effect on somatic EPSPs, bath application of TTX did not affect the peak amplitude of dendritic EPSPs; however, it reduced the integral of the largest subthreshold dendritic EPSPs. TTX also linearized the relationship between dendritic EPSP integral and the size of the current injection used to generate simulated EPSPs.

Bath application of TTX also blocked the amplification of small (<5 mV) somatic EPSPs evoked at depolarized membrane potentials (Figures 6C and 6D; n = 8). As with large EPSPs, TTX caused a greater reduction in EPSP integral than in EPSP peak amplitude (Figure 6D), decreasing the peak amplitude of somatic EPSPs recorded at the most depolarized subthreshold membrane potentials by 41% ± 2% and their integral by 80% ± 2% (n = 9). In the presence of TTX, the peak amplitude and integral of somatic EPSPs at the most depolarized membrane potentials were similar to the control EPSP amplitude and integral at the RMP (n = 9). In contrast to its effects on somatic EPSPs, the amplitude of dendritic EPSPs at depolarized membrane potentials was unchanged in the presence of TTX, despite a reduction in EPSP integral.

In summary, these results show that amplification of simulated EPSPs is largely, if not completely, blocked by TTX, indicating that it is mediated primarily by voltage-activated sodium channels. In addition, that TTX had no effect on the amplitude of dendritic EPSPs suggests that the peak of dendritic EPSPs is not amplified by voltage-activated sodium channels.

### Effects of Calcium Channel Blockers on Simulated EPSPs

To investigate the possibility that voltage-activated calcium channels are also involved in EPSP amplification, the effect of bath application of different calcium channel blockers on simulated EPSPs was determined. Unlike the experiments with TTX, the results from these experiments depended on the age of the animals used. In experiments on 28-day-old rats, $CdCl_2$ (200 μM; n = 3), $CoCl_2$ (2 mM; n = 4), and $NiCl_2$ (200 μM; n = 3) had no significant effect on simulated EPSPs during either an increase in EPSP amplitude or depolarization of the membrane potential. That calcium channels were blocked in these experiments was verified for $CdCl_2$ and $CoCl_2$ by their complete and rapid block of synaptic transmission. In 14-day-old rats, however, $CoCl_2$ (2 mM; n = 6) and $NiCl_2$ (200 μM; 5 out of 6 cells) caused a decrease in the amplitude and integral of the largest subthreshold simulated EPSPs, whereas $CdCl_2$ (200 μM; n = 5) had inconsistent effects (sometimes

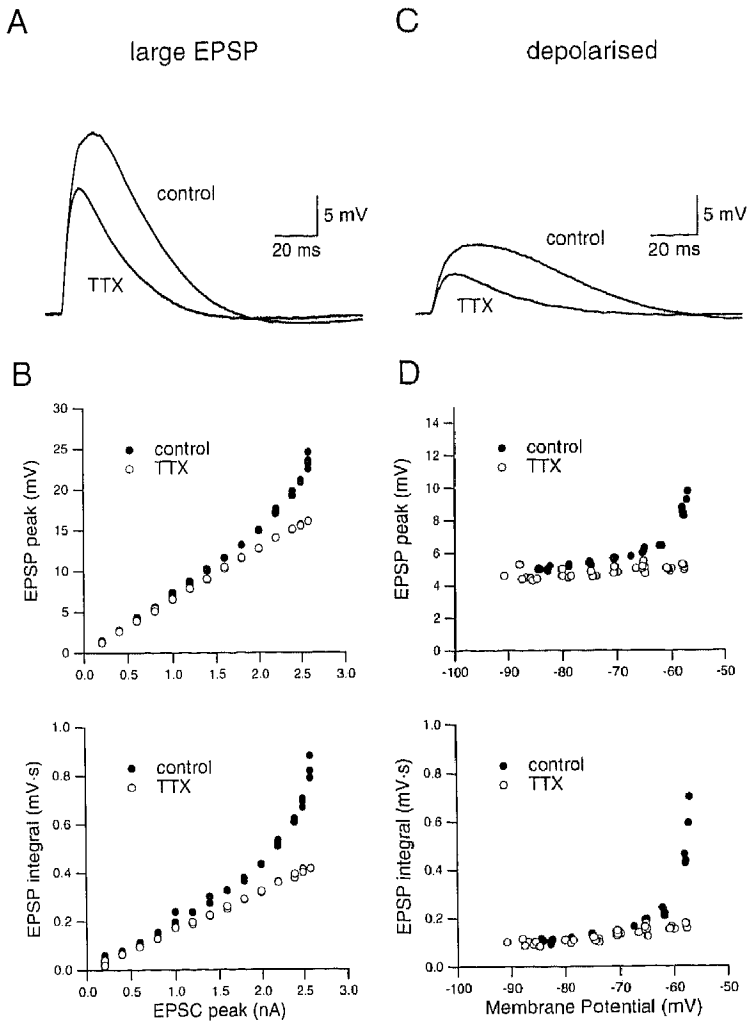


Figure 6. Effect of Bath Application of TTX on Simulated EPSPs

(A) The effect of bath application of tetrodotoxin (TTX) on large simulated EPSPs recorded at the soma at the RMP (−65 mV). Simulated EPSPs were generated by 2.6 nA dendritic current injections 330 μm from the soma.

(B) Plot of simulated EPSP peak amplitude (top) and integral (bottom) at the soma against the size of the dendritic current injection in the absence (closed circles) and presence (open circles) of TTX (data from same cell as in [A]).

(C) Effect of bath application of TTX on simulated EPSPs recorded at the soma at a depolarized membrane potential of −57 mV. Simulated EPSPs were generated by 1 nA dendritic current injections 450 μm from the soma; the somatic RMP was −65 mV.

(D) Plot of simulated EPSP peak amplitude (top) and integral (bottom) at the soma against the membrane potential at which the data were recorded in the absence (closed circles) and presence (open circles) of TTX (data from same cell as in [C]).

causing an increase [n = 3] and sometimes no change [n = 2]). On average, in 14-day-old rats $CoCl_2$ and $NiCl_2$ were less effective than TTX in reducing amplification of the largest subthreshold EPSPs, decreasing the peak amplitude of these simulated EPSPs by 19% ± 3% and their integral by 35% ± 4% (n = 6). The addition of TTX in the presence of $CoCl_2$ caused a further reduction in EPSP peak amplitude and integral (n = 4), whereas addition of $CoCl_2$ in the presence of TTX was largely without effect (small decrease in 2 out of 4 cells). In contrast to its effects on large EPSPs, in 14-day-old rats none of the calcium channel blockers had any effect on amplification of EPSPs at depolarized membrane potentials (n = 7). These results suggest that in older animals voltage-activated calcium channels are not involved in EPSP amplification; however, they may mediate a small component of EPSP amplification during large subthreshold EPSPs in young rats.

### Location of Sodium Channels Involved in EPSP Amplification

As suggested above, the site of somatic EPSP amplification is likely to be close to the soma. This possibility was tested by the local application of TTX to either the site of simulated EPSP generation in the dendrites or to the somatic region and axon. Local application of TTX was achieved by pressure ejection of TTX from a patch pipette, the tip of which was placed close to (<20 μm) either the dendritic recording site or the soma (usually close to the axon initial segment). The area perfused with TTX was determined by observing the spread of the dye Fast Green, included in the TTX solution, and was estimated to be ~50–100 μm in diameter. To minimize the spread of this TTX application, we used 100 nM TTX, a 10-fold lower concentration than was used for bath application (usually 1 μM). Spread of TTX was further reduced by the use of fast flow rates (5 ml/min) and an experimental chamber with a small bath volume (<1 ml). When TTX was applied to both the somatic and dendritic recording site of the same cell, the application of TTX was always made to the dendritic recording site first.

Local application of TTX to the dendritic recording site had little or no effect on amplification of somatic EPSPs during the largest subthreshold simulated EPSPs or small simulated EPSPs generated at depolarized membrane potentials (Figure 7A). That this TTX application did in fact

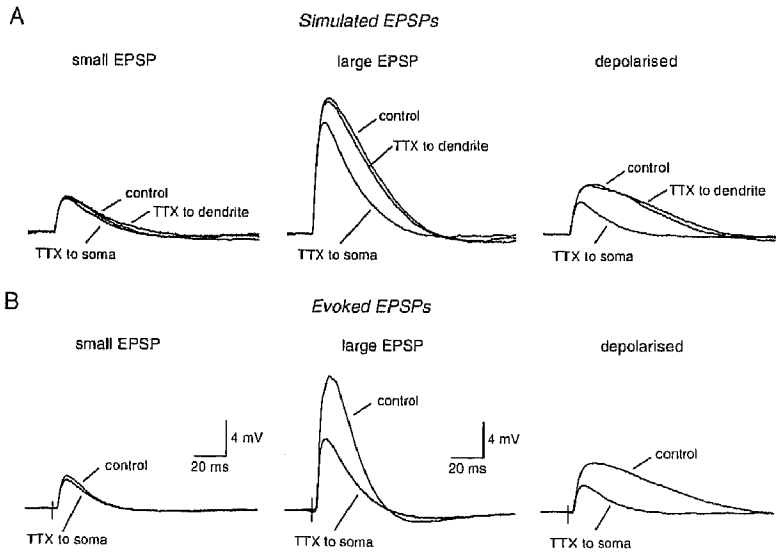


Figure 7. Effect of Local Application of TTX on Simulated and Evoked EPSPs

(A) Effect of local application of TTX to either the dendritic recording site or the soma and axon on small (left) and large (middle) simulated EPSPs at the RMP (−63 mV) and on small simulated EPSPs generated at a depolarized membrane potential of −53 mV (right). All recordings are from the soma of the same cell. Simulated EPSPs were generated by dendritic current injection 240 μm from the soma and were 0.5 nA (left and right traces) and 1.6 nA (middle traces). Scale is the same as in (B).

(B) Effect of local application of TTX to the soma and axon on small (left) and large (middle) evoked EPSPs at the RMP (−64 mV) and on small evoked EPSPs at a depolarized membrane potential of −53 mV (right). All recordings are from the soma of the same cell. The stimulus strength used to generate small EPSPs at the resting (left) and depolarized (right) membrane potentials was the same.

block dendritic sodium channels was verified by its ability to reduce the amplitude of back-propagating dendritic action potentials (see Stuart and Sakmann, 1994). In contrast, application of TTX to the soma and axon of the same cells reduced the somatic EPSP peak amplitude and integral of both large (>10 mV) and small (<5 mV) simulated EPSPs generated at depolarized membrane potentials, with little effect on small EPSPs at the RMP (Figure 7A). On average, application of TTX to the soma and axon reduced the peak amplitude of the largest subthreshold somatic EPSPs by 24% ± 3% and their integral by 45% ± 5% (n = 6), whereas at the most depolarized subthreshold membrane potentials, the somatic EPSP peak amplitude was reduced by 35% ± 3% and the integral by 72% ± 3 % (n = 5).

To determine whether amplification of evoked EPSPs can also be blocked by local application of TTX to the soma and axon, the effects of somatic and axonal TTX application on large subthreshold evoked EPSPs and small evoked EPSPs at depolarized membrane potentials were investigated. Similar to its effects on amplification of simulated EPSPs, this somatic and axonal application of TTX reduced the somatic peak amplitude and integral of large (>10 mV) and small (<5 mV) evoked EPSPs recorded at depolarized membrane potentials, with little effect on small EPSPs at the RMP (Figure 7B). On average, application of TTX to the soma and axon reduced the somatic peak amplitude of the largest subthreshold evoked EPSPs by 32% ± 3% and their integral by 43% ± 3% (n = 9), whereas at the most depolarized subthreshold membrane potentials, the somatic EPSP peak amplitude was reduced by 34% ± 5% and the integral by 80% ± 3% (n = 10). The fact that the same TTX application had little or no effect on the amplitude or integral of small (<5 mV) evoked EPSPs at the RMP (see Figure 7B) suggests that the block of evoked EPSP amplification by the local application of TTX to the soma and axon was not due to a presynaptic effect of TTX on transmitter release. In summary, these results show that local application of TTX to the soma and axon is sufficient to block amplification of both simulated and evoked somatic EPSPs, indicating that the voltage-activated sodium channels mediating somatic EPSP amplification are located close to the soma.

To investigate the possibility that amplification of EPSPs occurs in the axon, simultaneous somatic and axonal recordings were made from the same cells (axonal recordings were made 16–28 μm from the soma), and EPSPs were evoked either at different stimulus intensities or at different membrane potentials. In all cases (n = 5), while small (<5 mV) EPSPs at the RMP were almost identical at the somatic and axonal recording sites, the amplitude and integral of the largest subthreshold EPSPs and of EPSPs at the most depolarized subthreshold membrane potentials were larger in the axon (Figure 8).

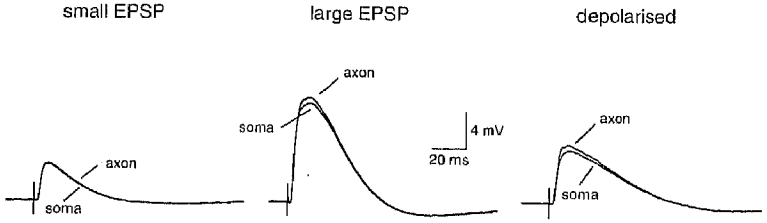


Figure 8. Comparison of EPSP Amplification in the Soma and Axon

Small (left) and large (middle) evoked EPSPs at the RMP (−64 mV) and small evoked EPSPs at a depolarized membrane potential of −57 mV (right) were recorded simultaneously at the soma and axon of the same cell (axonal recording 23 μm from the soma). The stimulus strength used to generate small EPSPs at the resting (left) and depolarized (right) membrane potentials was the same.

## Discussion

The results presented here show that subthreshold somatic EPSPs in neocortical layer V pyramidal neurons can be amplified by voltage-activated channels. EPSP amplification occurred for large EPSPs (>5 mV) or EPSPs evoked at depolarized membrane potentials and is mediated by the activation of voltage-activated sodium channels located close to the soma and in the axon.

### Conductances Involved in Amplification of EPSPs

The TTX sensitivity and slow time course of EPSP amplification suggest that it is mediated by voltage-activated sodium channels of the persistent sodium channel type ($I_{NaP}$). A role for $I_{NaP}$ in amplification of somatic EPSPs at depolarized membrane potentials was first proposed by Stafstrom et al. (1985; see also Sutor and Hablitz, 1989a, 1989b; Deisz et al., 1991; Hirsch and Gilbert, 1991). We show here that EPSPs with amplitudes of >5 mV at the RMP are also amplified by voltage-activated sodium channels, presumably also of the $I_{NaP}$ type. As $I_{NaP}$ channels can be activated at membrane potentials hyperpolarized to action potential threshold (Stafstrom et al., 1985; Brown et al., 1994), this makes them ideally suited to amplify subthreshold EPSPs.

The possibility that calcium channels were also involved in amplification of EPSPs was tested by bath application of various calcium channel blockers. Subthreshold EPSPs have previously been shown to generate an increase in intracellular calcium in layer V pyramidal neurons following the activation of voltage-dependent calcium channels (Markram and Sakmann, 1994). In addition, a study in pyramidal neurons in layer 2/3 of the neocortex concluded that amplification of EPSPs at depolarized membrane potentials is largely mediated by voltage-activated calcium channels (Deisz et al., 1991). The results presented here suggest that in older animals (28 days) the activation of voltage-dependent calcium channels by subthreshold EPSPs does not contribute significantly to the voltage change that occurs during a somatic EPSP in layer V neurons. In young animals (14 days), however, large (>5 mV) simulated EPSPs were reduced by $CoCl_2$ and $NiCl_2$ but not by $CdCl_2$. This result suggests that these EPSPs are amplified by voltage-activated calcium channels. The extent of this amplification, however, was smaller than that mediated by voltage-activated sodium channels, was restricted only to amplification of large EPSPs, and was absent in 28-day-old rats. The reasons for the differential effects of the different calcium channel blockers on large subthreshold simulated EPSPs in 14- and 28-day-old rats are not clear, but it may suggest a developmental change in the expression of different classes of calcium channels in layer V pyramidal neurons during the first 4 postnatal weeks (but see Lorenzon and Foehring, 1995).

The different effects of the calcium channel blockers in 14- and 28-day-old animals are unlikely to be due to "washout" of calcium current in the older animals, as this would presumably be similar in recordings from animals at both ages. Further evidence against the idea that washout of calcium conductances occurred in our experiments comes from the fact that a substantial calcium component following dendritic action potentials could be observed, which was particularly large during somatic action potential burst firing (see Amitai et al., 1993; Kim and Connors, 1993). This suggests that, under the experimental conditions used in the present study, dendritic calcium conductances were intact. Finally, similar results were obtained in experiments with widely varying series resistances (between 5 and 100 MΩ), where the extent of washout should be very different, and no change in the extent of EPSP amplification was detected during recordings that could last up to 1 hr or more.

### Location of the Conductances Involved in EPSP Amplification

Many aspects of the data suggest that the conductances involved in EPSP amplification are located close to the soma. First, subtraction of somatic and dendritic EPSPs at the RMP from those at depolarized membrane potentials showed that during these recordings EPSP amplification was largest at the soma (see Figure 5B). Second, local application of TTX to the soma and axon blocked EPSP amplification of both simulated and evoked EPSPs (see Figure 7). Finally, simultaneous somatic and axonal recordings showed that EPSP amplification was in fact largest in the initial part of the axon (see Figure 8). Together, these results show that the voltage-activated sodium channels that mediate EPSP amplification are located near the soma and in the axon.

As EPSP amplification is mediated primarily by $I_{NaP}$, the location of the $I_{NaP}$ channels involved in EPSP amplification must also be located near the soma and in the axon. Recent studies in neocortical pyramidal neurons (Alzheimer et al., 1993) suggest that the sodium channels mediating $I_{NaP}$ are the same channels as those generating the action potential but have switched into a "noninactivating" gating mode. Alzheimer et al. (1993) predicted that ~0.1% of all sodium channels enter into this noninactivating gating mode and so could contribute to $I_{NaP}$. Given this result, it is perhaps not surprising that EPSP amplification was largest in the axon, the site of presumably the highest sodium channel density.

### Can EPSPs Be Amplified by Dendritic Voltage-Activated Channels?

It has been postulated that EPSPs may be amplified by dendritic voltage-activated channels, possibly in spines (see Jack et al., 1983; Miller et al., 1985; Perkel and Perkel, 1985; Cauller and Connors, 1992; De Schutter and Bower, 1994; Bernander et al., 1994). In support of this idea, large subthreshold EPSPs have recently been shown to activate sodium and calcium channels in dendritic cell-attached patches from hippocampal pyramidal neurons (Magee and Johnston, 1995), and calcium imaging experiments have shown that subthreshold EPSPs can evoke dendritic calcium transients due to the activation of dendritic voltage-activated calcium channels in neocortical pyramidal (Mar-

kram and Sakmann, 1994) and cerebellar (Eilers et al., 1995) Purkinje neurons. Together, these studies suggest that dendritic voltage-dependent channels can be activated by subthreshold EPSPs; however, they do not indicate the extent to which this will lead to amplification of the voltage change during these EPSPs.

The results presented in the present study suggest that any amplification of EPSPs by voltage-activated channels in the apical dendrite, or in spines on the apical dendrite, of neocortical layer V pyramidal neurons must be small in comparison to that which occurs close to the soma. This conclusion is based on the following evidence. Owing to their small capacitance and short electrotonic length, the voltage experienced by dendritic spines close to the dendritic recording pipette will be similar to that in the adjacent dendrite (see Jack et al., 1983). This dendritic voltage change during the largest subthreshold simulated EPSPs was up to 50 mV in amplitude (see Figure 4), which should be of sufficient size to activate most voltage-activated sodium and calcium channels. Yet the peak amplitude of dendritic simulated EPSPs increased linearly with the amplitude of the dendritic current injection (Figure 4B) and was unaffected by application of sodium or calcium channel blockers. In addition, application of TTX to the site of generation of dendritic simulated EPSPs had little or no effect on the amplitude or duration of simulated EPSPs, whereas EPSP amplification could be blocked by application of TTX to the soma and axon (see Figure 7). Together, these results suggest that dendritic voltage-activated channels in the apical dendrite, or those in neighboring spines, are at such a low density that their activation does not significantly amplify dendritic EPSPs under the recording conditions of our study. That the dendritic EPSP integral, but not the peak, is amplified during the largest subthreshold EPSPs and at depolarized membrane potentials (see Figures 4 and 5) presumably results from the passive spread of EPSP amplification at the soma back to the dendritic recording site.

It should be noted that the conclusions from these experiments are restricted to EPSPs made onto the main apical dendrite of layer V pyramidal neurons. This leaves open the possibility that EPSPs in the more distal dendrites may under some circumstances be amplified locally by dendritic voltage-activated channels. However, the ability of simulated EPSPs to mimic adequately the evoked EPSPs, together with the finding that local application of TTX to the soma and axon blocked amplification of both simulated and evoked EPSPs, suggests that, if local amplification of distal EPSPs by dendritic voltage-activated channels does occur, this does not significantly amplify the somatic membrane potential in comparison with that which occurs following EPSP amplification by voltage-activated sodium channels located close to the soma.

### Physiological Significance of EPSP Amplification for Synaptic Integration

The amplification of subthreshold EPSPs by voltage-activated sodium channels located near the soma and in the axon has implications for synaptic integration in neocortical layer V pyramidal neurons. EPSPs were not significantly amplified when evoked from the RMP unless they were at least 5 mV in amplitude at the soma, and often needed to be closer to 10 mV. While EPSPs of this amplitude are easily achieved during synchronized extracellular stimulation, are they likely to occur under more physiological conditions in vivo? One possibility is that in neocortical pyramidal neurons large compound EPSPs may be evoked during synchronized burst firing of neighboring pyramidal neurons.

Amplification of EPSPs at depolarized membrane potentials could be observed for very small EPSPs (1–2 mV). In addition, unitary EPSPs, evoked by action potentials in neighboring pyramidal neurons, are also amplified in amplitude and duration by depolarization of the membrane potential (G. S., unpublished data; see also Thomson et al., 1988). This suggests that EPSP amplification at depolarized membrane potentials may be of more significance to synaptic integration than EPSP amplification by large EPSPs evoked from a negative RMP.

An interesting property of EPSP amplification is that it is associated with a greater increase in EPSP integral than in peak amplitude, and hence will increase the time window over which temporal summation of EPSPs can occur. In addition, this has the consequence that action potentials evoked by just threshold EPSPs, especially at depolarized membrane potentials, are evoked at some time (often tens of milliseconds) after the onset of the EPSP (see Figure 3A), with the actual time of action potential initiation by these EPSPs depending on the extent and time course of EPSP amplification. It could be argued that these findings are counterintuitive, as one might expect that the temporal information contained in the peak of an EPSP should be conserved by the neuron. It is worth noting, however, that neurons which are responsible for conveying temporal information (e.g., in the auditory pathway) have few or no dendrites and fast, very large single fiber EPSPs (see Zhang and Trussell, 1994). Perhaps in neocortical pyramidal neurons temporal information may be conveyed more by the rate of action potential firing, rather than by the precise timing of each action potential (Shadlen and Newsome, 1994; but see Hopfield, 1995).

As the results suggest that EPSPs are not amplified locally by dendritic voltage-activated channels, the question arises as to whether there are other mechanisms that enhance the ability of distal EPSPs to influence action potential initiation. Perhaps the quantal size of distal EPSPs is larger than that of more proximal EPSPs (Jack et al., 1981), or distal synapses have a higher probability of transmitter release. It should also be noted that while passive cable theory predicts significant attenuation of the peak of distal EPSPs as they spread to the soma, the EPSP integral will not be attenuated to the same extent (Jack et al., 1983; compare Figures 4B and 4C). As it has been suggested that an EPSP integral is a more important determinant of whether an EPSP will initiate an action potential than its peak amplitude (Jack et al., 1983), the ability of distal EPSPs to initiate action potentials will be greater than that predicted simply by the attenuation of an EPSP's peak amplitude. Finally, the amplification of EPSPs by voltage-activated sodium channels located

close to the soma and in the axon will further enhance the ability of distal EPSPs to influence action potential initiation.

### Experimental Procedures

Experiments were performed on 300 μm thick sagittal brain slices from somatosensory cortex of 14- to 28-day-old Wistar rats using previously described techniques (Stuart et al., 1993; Sakmann and Stuart, 1995). Slices were perfused continuously with an oxygenated Ringer solution containing 125 mM NaCl, 25 mM $NaHCO_3$, 25 mM glucose, 2.5 mM KCl, 1.25 mM $NaH_2PO_4$, 2 mM $CaCl_2$, and 1 mM $MgCl_2$ (pH 7.4 with 5% $CO_2$); all experiments were performed at 35°C ± 1°C. Pooled data are expressed as the mean ± SEM, and no correction for the junction potential between the bath and pipette solutions was made. Full correction for this junction potential would make all membrane potential measurements −12 mV more negative than indicated.

#### Recording of Spontaneous EPSCs

Whole-cell voltage-clamp recordings (uncompensated series resistance 4–7 MΩ) of spontaneous EPSCs were made from the soma of visually identified layer V pyramidal neurons using an EPC-7 patch-clamp amplifier (List, Darmstadt, Germany) in the presence of bicuculline methiodide (20 μM; Sigma) to block $GABA_A$ inhibitory synaptic events. Patch pipettes were filled with the following intracellular solution: 120 mM K-gluconate, 20 mM KCl, 10 mM HEPES, 10 mM EGTA, 2 mM $Na_2$-ATP, and 2 mM $MgCl_2$ (pH 7.3). Spontaneously occurring EPSCs at the RMP were filtered at 2 kHz and sampled at 50 kHz using a VME bus computer (Motorola Delta series 1147, Tempe, Arizona). For each cell an average was compiled from 50–200 events with 20%–80% rise times of <0.5 ms and decays uncontaminated by other spontaneous events. The assumption was that the fastest rising events will be the best space-clamped, so their time course will most closely represent the true time course of the EPSC.

#### Current-Clamp Recordings of Evoked and Simulated EPSPs

Whole-cell current-clamp recordings (seal resistances > 5 GΩ) were made from the soma and dendrites or soma and axon of visually identified layer V pyramidal neurons using two identical microelectrode amplifiers (Axoclamp 2A, Axon Instruments). Voltage was filtered at 10 kHz and sampled at 50 or 10 kHz using a VME bus computer. Patch pipettes (4–7 MΩ for somatic recordings, 8–10 MΩ for dendritic recordings, 10–12 MΩ for axonal recordings) were filled with the same K-gluconate-based intracellular solution as described above, and recordings were terminated if the access resistance exceeded 100 MΩ. That dendritic or axonal recordings were in fact made from the dendrites or axon has been confirmed in previous studies by the use of the fluorescent dye Lucifer Yellow (see Sakmann and Stuart, 1995). The distance of dendritic recordings from the soma was measured from the center of the soma, whereas the distance of axonal recordings from the soma was measured from the axon hillock. All measurements were made directly from the video monitor using the Argus 10 system (Hamamatsu, Hamamatsu City, Japan).

Monosynaptic EPSPs were evoked by 200 μs pulses (up to 30 V in amplitude) applied to an extracellular stimulating pipette usually placed in layer 2/3. This stimulation pipette was made from a fire-polished patch pipette with a tip diameter of ~10 μm filled with oxygenated Ringer solution. Unless otherwise stated, all experiments with synaptic stimulation were performed in APV (50 μM; Tocris, England) and bicuculline (20 μM; Sigma) to block NMDA and $GABA_A$ receptors. Epileptic discharges were observed in the presence of bicuculline; however, the frequency of epileptic discharges and polysynaptic components during EPSPs was reduced when $GABA_A$ antagonists were used in conjunction with NMDA antagonists. Records where clear polysynaptic components occurred during EPSPs were rejected from analysis.

Simulated EPSPs were generated by injection of an exponentially rising and falling voltage waveform ($\tau_{on}$ = 0.3 ms; $\tau_{off}$ = 3 ms) into the current-clamp input of the Axoclamp amplifier used to make the dendritic recording (dendritic current injections were made 170–580 μm from the soma). When required, the size of the dendritic current injection was varied by scaling the amplitude of this voltage waveform. Inverted current injections were used to control for changes in either the current-passing abilities of the dendritic recording pipette or the condition of the cell. The results from experiments where significant changes in the somatic response to this inverted waveform were observed during the course of the experiment were discarded. Accurate bridge and capacitive compensation are essential if the voltage change at the site of the dendritic current injection is to be trusted. For this reason, the voltage change at the dendritic recording pipette during a simulated EPSP was used for analysis only if the dendritic access resistance was <30 MΩ, was stable, and could be adequately compensated.

Two different methods were used to investigate amplification of evoked and simulated EPSPs. Either the amplitude of EPSPs was changed, by altering the stimulus strength for evoked EPSPs or the size of the dendritic current injection for simulated EPSPs, or small (<5 mV at the soma at the RMP) evoked or simulated EPSPs, generated at the same stimulus strength or size of dendritic current injection, were examined at different membrane potentials. In these experiments, evoked or simulated EPSPs were initiated 500 ms after depolarizing or hyperpolarizing current pulses were applied to either the soma or dendrite, or both. When bath applied, TTX, $CdCl_2$, CsCl, and $NiCl_2$ were added directly to the Ringer solution to give the concentrations indicated. In experiments using $CoCl_2$, $CaCl_2$ and $NaH_2PO_4$ were removed, and 2 mM $CoCl_2$ was added. For experiments involving the local application of TTX, TTX (100 nM) was dissolved in freshly oxygenated Ringer solution together with 0.2% Fast Green (Sigma) and placed in a patch pipette with a tip diameter of ~2 μm. Ejection of TTX from this pipette was achieved by the application of pressure to the back of this pipette by mouth or from a syringe.

### Acknowledgments

We thank Michael Häusser, Guy Major, Jackie and Izik Schiller, and Nelson Spruston for their comments on earlier versions of the manuscript. G. S. acknowledges the financial support of the Alexander von Humboldt Stiftung.

The costs of publication of this article were defrayed in part by the payment of page charges. This article must therefore be hereby marked *"advertisement"* in accordance with 18 USC Section 1734 solely to indicate this fact.

Received July 28, 1995; revised September 25, 1995.

### References

Alzheimer, C., Schwindt, P.C., and Crill, W.E. (1993). Modal gating of $Na^+$ channels as a mechanism of persistent $Na^+$ current in pyramidal neurons from rat and cat sensorimotor cortex. J. Neurophysiol. *13*, 660–673.

Amitai, Y., Friedman, B., Connors, B.W., and Gutnick, M.J. (1993). Regenerative activity in apical dendrites of pyramidal cells in neocortex. Cereb. Cortex *3*, 26–38.

Artola, A., and Singer, W. (1990). The involvement of N-methly-D-aspartate receptors in induction and maintenance of long-term potentiation in rat visual cortex. Eur. J. Neurosci. *2*, 254–269.

Bernander, O., Koch, C., and Douglas, R.J. (1994). Amplification and linearization of distal synaptic input to cortical pyramidal cells. J. Neurophysiol. *72*, 2743–2753.

Brown, A.M., Schwindt, P.C., and Crill, W.E. (1994). Different voltage dependence of transient and persistent $Na^+$ currents is compatible with modal-gating hypothesis for sodium channels. J. Neurophysiol. *71*, 2562–2565.

Cauller, L.J., and Connors, B.W. (1992). Functions of very distal dendrites: experimental and computational studies of layer I synapses on neocortical pyramidal cells. In Single Neuron Computation, T. McKenna, J. Davis, and S. F. Zornetzer, eds. (Boston, Massachusetts: Academic Press), pp. 199–229.

Chagnac-Amitai, Y., Luhmann, H.J., and Prince, D.A. (1990). Burst generating and regular spiking layer 5 pyramidal neurons of rat neocortex have different morphological features. J. Comp. Neurol. *296*, 598–613.

Deisz, R.A., Fortin, G., and Zieglgänsberger, W. (1991). Voltage-dependence of excitatory postsynaptic potentials of rat neocortical pyramidal neurons. J. Neurophysiol. *65*, 371–382.

De Schutter, E., and Bower, J.M. (1994). Simulated responses of cerebellar Purkinje cells are independent of the dendritic location of granule cell synaptic inputs. Proc. Natl. Acad. Sci. USA *91*, 4736–4740.

Eilers, J., Augustine, G.J., and Konnerth, A. (1995). Subthreshold synaptic $Ca^{2+}$ signalling in fine dendrites and spines of cerebellar Purkinje neurons. Nature *373*, 155–159.

Hirsch, J., and Gilbert, C.D. (1991). Synaptic physiology of horizontal connections in the cat visual cortex. J. Neurophysiol. *11*, 1800–1809.

Hopfield, J.J. (1995). Pattern recognition computation using action potential timing for stimulus representation. Nature *376*, 33–36.

Huguenard, J.R., Hamill, O.P., and Prince, D.A. (1989). Sodium channels in dendrites of rat cortical pyramidal neurons. Proc. Natl. Acad. Sci. USA *86*, 2473–2477.

Jack, J.J.B., Redman, S.J., and Wong, K. (1981). The components of synaptic potentials evoked in cat spinal motoneurones by impulses in single group Ia afferents. J. Physiol. *321*, 65–96.

Jack, J.J.B., Noble, D., and Tsien, R.W. (1983). Electrical Current Flow in Excitable Cells (Oxford: Oxford University Press).

Jones, K.A., and Baughman, R. (1988). NMDA- and non-NMDA-receptor components of excitatory synaptic potentials recorded from cells in layer V of rat cortex. J. Neurosci. *8*, 3522–3534.

Kasper, E.M., Larkman, A.U., Lübke, J., and Blakemore, C. (1994). Pyramidal neurons in layer 5 of the rat visual cortex. II. Development of electrophysiological properties. J. Comp. Neurol. *339*, 475–494.

Kim, H.G., and Connors, B.W. (1993). Apical dendrites of the neocortex: correlation between sodium- and calcium-dependent spiking and pyramidal cell morphology. J. Neurosci. *13*, 5301–5311.

Lorenzon, N.M., and Foehring, R.C. (1995). Characterization of pharmacologically identified voltage-gated calcium currents in acutely isolated rat neocortical neurons. II. Postnatal development. J. Neurophysiol. *73*, 1443–1451.

Magee, J.C., and Johnston, D. (1995). Synaptic activation of voltage-gated channels in the dendrites of hippocampal pyramidal neurons. Science *268*, 301–304.

Markram, H., and Sakmann, B. (1994). Calcium transients in dendrites of neocortical neurons evoked by single subthreshold excitatory postsynaptic potentials via low-voltage-activated calcium channels. Proc. Natl. Acad. Sci. USA *91*, 5207–5211.

Markram, H., Helm, P.J., and Sakmann, B. (1995). Dendritic calcium transients evoked by single back-propagating action potentials in rat neocortical pyramidal neurones. J. Physiol. *485*, 1–20.

Mason, A., and Larkman, A. (1990). Correlations between morphology and electrophysiology of pyramidal neurons in slices of rat visual cortex. II. Electrophysiology. J. Neurosci. *10*, 1415–1428.

Miller, J.P., Rall, W., and Rinzel, J. (1985). Synaptic amplification by active membrane in dendritic spines. Brain Res. *325*, 325–330.

Perkel, D.H., and Perkel, D.J. (1985). Dendritic spines: role of active membrane in modulating synaptic efficacy. Brain Res. *325*, 331–335.

Rall, W. (1977). Core conductor theory and cable properties of neurons. In Handbook of Physiology. The Nervous System, Vol. 1, part 1, E. R. Kandel, ed. (Bethesda, Maryland: American Physiological Society), pp. 39–97.

Regehr, W., Kehoe, J., Ascher, P., and Armstrong, C. (1993). Synaptically triggered action potentials in dendrites. Neuron *11*, 145–151.

Sakmann, B., and Stuart, G. (1995). Patch-pipette recordings from the soma, dendrites and axon of neurons in brain slices. In Single Channel Recording, B. Sakmann and E. Neher, eds. (New York: Plenum Press), pp. 199–211.

Schiller, J., Helmchen, F., and Sakmann, B. (1995). Spatial profile of dendritic calcium transients evoked by action potentials in rat neocortical pyramidal neurons. J. Physiol. *487*, 583–600.

Shadlen, M., and Newsome, W. (1994). Noise, neural codes and cortical organization. Curr. Opin. Neurobiol. *4*, 569–579.

Stafstrom, C.E., Schwindt, P.C., Flatman, J.A., and Crill, W.E. (1984). Properties of subthreshold response and action potential recorded in layer V neurons from cat sensorimotor cortex *in vitro*. J. Neurophysiol. *52*, 244–263.

Stafstrom, C.E., Schwindt, P.C., Chubb, M.C., and Crill, W.E. (1985). Properties of persistent sodium conductance and calcium conductance of layer V neurons from cat sensorimotor cortex *in vitro*. J. Neurophysiol. *53*, 153–170.

Stuart, G.J., and Sakmann, B. (1994). Active propagation of somatic action potentials into neocortical pyramidal cell dendrites. Nature *367*, 69–72.

Stuart, G.J., Dodt, H.-U., and Sakmann, B. (1993). Patch-clamp recordings from the soma and dendrites of neurones in brain slices using infrared video microscopy. Pflügers Arch. *423*, 511–518.

Sutor, B., and Hablitz, J.J. (1989a). EPSPs in rat neocortical neurons *in vitro*. I. Electrophysiological evidence for two distinct EPSPs. J. Neurophysiol. *61*, 607–620.

Sutor, B., and Hablitz, J.J. (1989b). EPSPs in rat neocortical neurons *in vitro*. II. Involvement of N-methyl-D-aspartate receptors in the generation of EPSPs. J. Neurophysiol. *61*, 621–634.

Thomson, A.M., Girdlestone, D., and West, D.C. (1988). Voltage-dependent currents prolong single-axon postsynaptic potentials in layer III pyramidal neurons in rat neocortical slices. J. Neurophysiol. *60*, 1896–1907.

Yuste, R., Gutnick, M.J., Saar, D., Delaney, K.R., and Tank, D.W. (1994). $Ca^{2+}$ accumulations in dendrites of neocortical pyramidal neurons: an apical band and evidence for two functional compartments. Neuron *13*, 23–43.

Zhang, S., and Trussell, L.O. (1994). A characterization of excitatory postsynaptic potentials in the avian nucleus magnocellularis. J. Neurophysiol. *72*, 705–718.